Graham & Chang (1965) have speculated from thermodynamic considerations that vitreous selenium quenched from 775°K has smaller average molecular weight than that quenched from 700°K. The results of this study suggest that quenching from different melt temperatures does not seem to affect significantly the nearest neighbor packing but may affect the configurational arrangement of atoms at larger radial distances. It is not believed possible at this stage, however, to relate the small differences in the radial density function from X-ray diffraction studies to the intermolecular structures in any quantitative way, although Richter & Herre (1958) have approached the problem by assuming the presence of layered structures to account for the presence of additional peaks in the radial density function. In order to attack the problem on a more quantitative basis, it is essential to improve further the accuracy of experimental data acquisition and to extend such data collection to lower as well as larger S values than those reached in this work.

The authors wish to thank Stephen T. Imrich, North American Aviation Science Center, for help on data reduction and programming details.

References

GRAHAM, L. J. & CHANG, R. (1965). *J. Appl. Phys.* **36**, 2983.
HENDUS, H. (1942). *Z. Physik*, **119**, 265.
HENNINGER, E. H., BUSCHERT, R. C. & HEATON, L. (1967). *J. Chem. Phys.* **46**, 586.
KAPLOW, R., STRONG, S. L. & AVERBACH, B. L. (1965). *Phys. Rev.* **138**, A1336.
LARK-HOROVITZ, K. & MILLER, E. P. (1937). *Phys. Rev.* **51**, 380.
RICHTER, H. & HERRE, F. (1958). *Z. Naturforsch.* **13** A, 874.
ZERNICKE, F. & PRINS, J. A. (1927). *Z. Physik*, **41**, 184.

Acta Cryst. (1967). **23**, 704

Study of Chrysotile Asbestos by a High Resolution Electron Microscope

BY KEIJI YADA

Research Institute for Scientific Measurements, Tohoku University, Sendai, Japan

(*Received* 22 *May* 1967 *and in revised form* 19 *July* 1967)

Microfibers of chrysotile asbestos were observed from two directions parallel and perpendicular to the fiber axis by selected area electron diffraction and high resolution electron microscopy. The results are as follows: (*a*) Most of the fibers have a hollow cylindrical form. Some fibers, however, are not hollow but solid, showing an unusual growth pattern. (*b*) Splitting of diffraction spots is observed with a highly parallel illumination. (*c*) The observed dislocation patterns suggest that the value of the *c* parameter is 7·3 Å rather than 14·6 Å. (*d*) The lattice image observed in the cross sections of fiber shows multi-spiral lattice fringes instead of concentric ones, in conformity with the hypothesis of Jagodzinski and Kunze.

Introduction

Since the first work by Warren & Bragg (1930), the crystal structures of chrysotile asbestos have been studied by many workers not only by X-ray diffraction but also by electron microscopy and electron diffraction (Warren & Herring, 1941; Aruja, 1943; Padurow, 1950; Bates, Hildebrand & Swineford, 1950; Whittaker, 1951; Brindley, 1952; Honjo & Mihama, 1954; Jagodzinski & Kunze, 1954*a*,*b*,*c*; Whittaker, 1954, 1955, 1956; Whittaker & Zussman, 1956; Zussman, Brindley & Comer, 1957). However, more detailed studies seem to be necessary concerning the form of microfibers, lattice parameters, and crystal growth mechanism.

The resolution of electron microscopes has been so markedly improved that nowadays it is possible to observe the lattice planes, as lattice fringes, of spacings in the 1·5–2 Å range when the crystalline specimens satisfy Bragg conditions appropriately and their thicknesses are suitable. The tilted illumination method had been recommended for such high resolution work (Dowell, 1963; Komoda, 1966). Recently, however, it has been shown that lattice resolution attained by the axial illumination method can be as high as that obtained with tilted illumination (Yada & Hibi, 1966), and, as a result, it becomes very easy to obtain the lattice images of isolated small specimens such as chrysotile fibers.

Fernández-Morán (1966) observed the lattice images on chrysotile fibers which were used as supporters of micro-organisms, and utilized the lattice fringes for the calibration of magnification. In the present work, microfibers of chrysotile were observed by means of a high resolution electron microscope in order to study the crystal structure and the crystal growth mechanism.

Specimen and experimental

The specimen used in the present work was micropulverized chrysotile from Jeffrey mine, Canada. Ac-

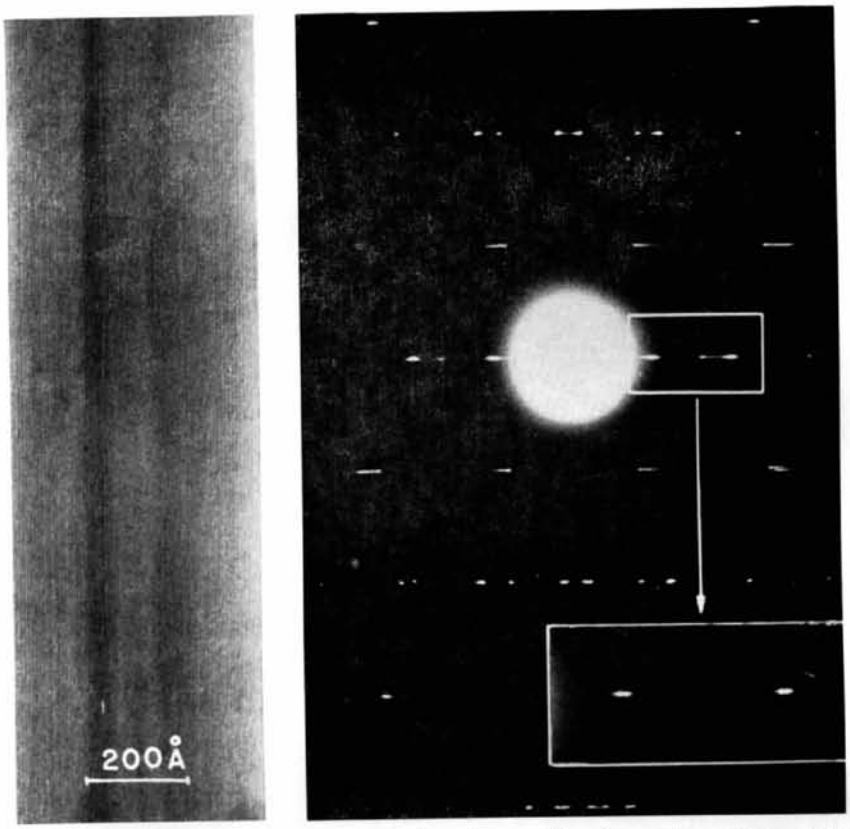

Fig. 1. Electron micrograph of a fiber of chrysotile and its selected area diffraction pattern. Some of the diffraction spots are split by the double refraction effect corresponding to the cylindrical form of the fiber. The enlarged pattern framed with a white line shows it more clearly.

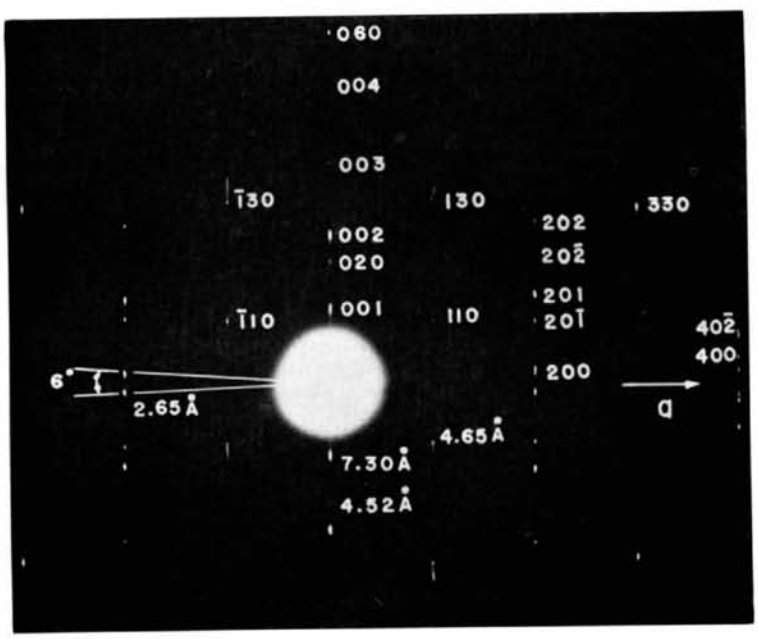

Fig. 2. Electron diffraction pattern of chrysotile with the indices of the diffraction spots and the values of the interplanar spacings.

[*To face p.*704

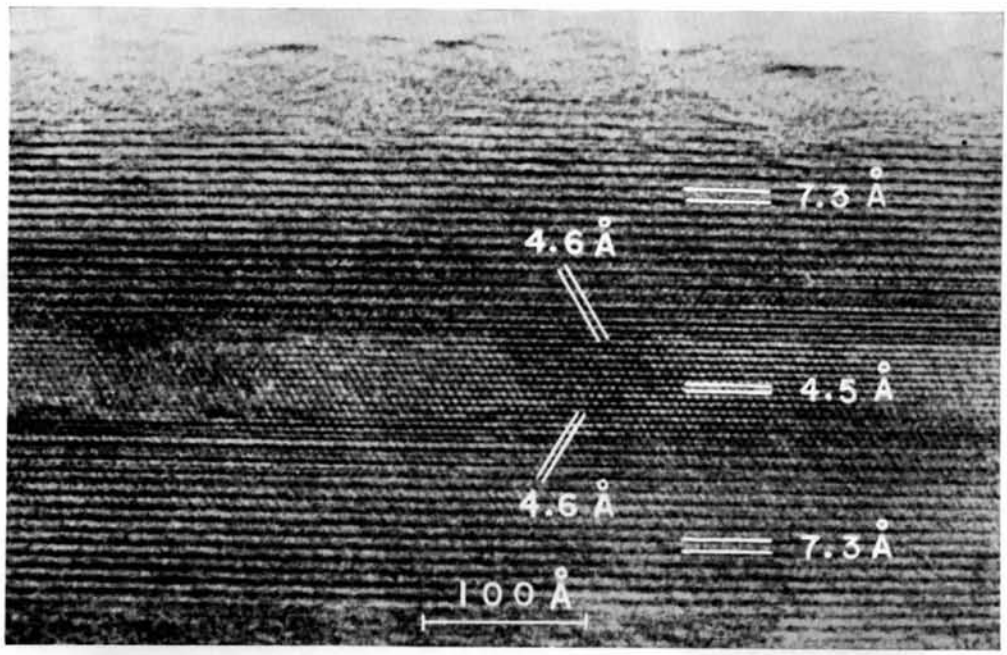

Fig. 3. A typical example of the lattice image in chrysotile observed from the direction perpendicular to the fiber axis.

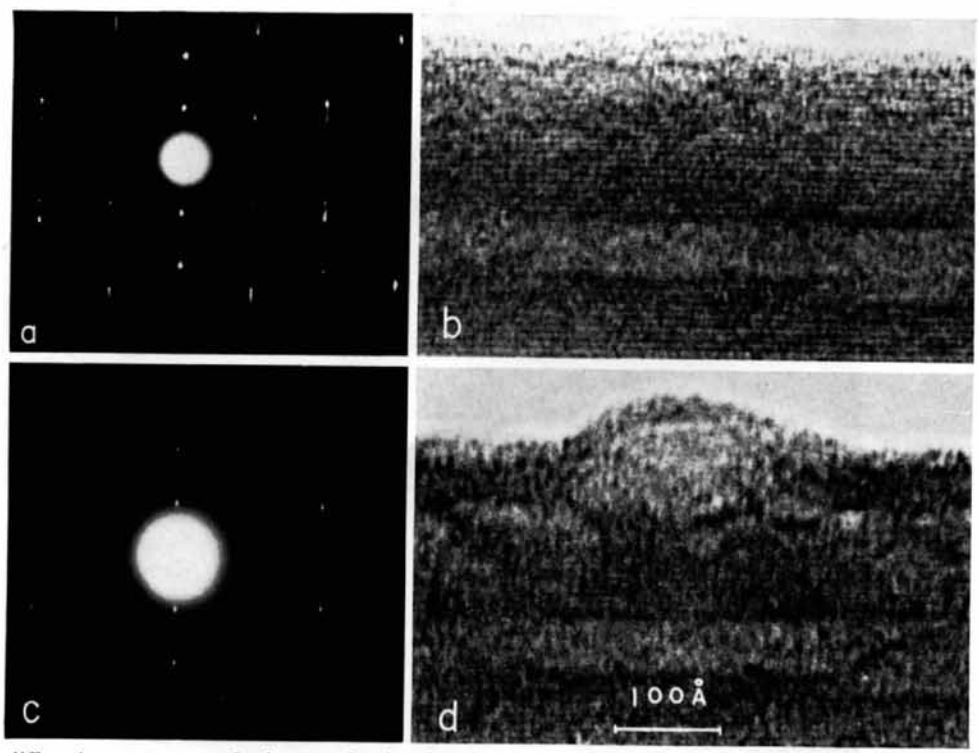

Fig. 4. Electron diffraction patterns and micrographs showing the electron beam irradiation effect on chrysotile fiber. The crystalline structure in the fresh specimen (*a* and *b*) changes to the amorphous state with intense electron irradiation (*c* and *d*).

cording to Whittaker (1956) it is thought that most of the fibers are clino-chrysotile.

The following two kinds of specimen preparation method were employed for electron microscopy.

(*a*) *Suspension method*

A small droplet of distilled water in which chrysotile fibers were suspended was dried in air on a microgrid reinforced with evaporated carbon. The fibers spanning the holes of the microgrid, and thus being without a supporting film, were subjected to observation.

(*b*) *Section method*

Chrysotile fibers embedded in methyl methacrylate were sectioned by means of an ultramicrotome with a diamond knife. Prior to this procedure, the fibers were successively rinsed with absolute ethanol, a mixture of ethanol and methyl methacrylate, and pure methyl methacrylate. The embedding plastic of thin sections (300–800 Å in thickness) mounted on thin carbon films was dissolved away with benzene before the electron-microscope observations were carried out, in order to avoid a loss of image contrast.

A Hitachi HU-11B electron microscope was used at 75 or 100 kV, with a pointed cathode. The illumination angle was about 5×10^{-4} radian at the employed electron optical magnification of 160,000–200,000. Specimen contamination during the observations was reduced to a negligible level by using an anti-contamination device for cooling the vicinity of the specimen holder, in addition to the standard device of HU-11B. The electron microscope operated under the optimum instrumental condition was capable of a lattice image resolution around 2 Å. Selected area diffraction patterns were taken with a higher parallel illumination ($\sim 5 \times 10^{-5}$ radian) than that in the imaging case. The interplanar spacings of chrysotile were found from the selected area diffraction pattern relative to diffraction rings of gold evaporated onto the chrysotile fibers.

Experimental results

Specimens prepared by the suspension method

It was found that the outer diameter of the microfibers ranges from about 150 to 1000 Å, the average value being about 500 Å.

Fig. 1 shows an electron micrograph of a fiber and its electron diffraction pattern. The lattice fringes of 7·3 Å spacing are seen parallel to the fiber axis. In the diffraction pattern, the splitting of each diffraction spot along the direction perpendicular to the fiber axis is observed, as shown in the enlarged part. The splitting seems to be attributable to the double refraction effect due to the cylindrical form of the fiber,* similarly to the splitting of spots in the case of cubic shaped crystals such as magnesium oxide smokes (see, *e.g.* Honjo, 1953).

The calibrated values of some interplanar spacings corresponding to the central positions of the split spots and the indices of diffraction spots are given in Fig. 2. Assuming the monoclinic structure of chrysotile, the value of β is determined to be 93° from the observed diffraction pattern. The values of the lattice parameters of chrysotile reported by previous workers and the present author are listed in Table 1. It is seen that the lattice parameters obtained here are in good agreement with those by Brindley (1952) and Jagodzinski & Kunze (1954*a*). The reason why 7·3 Å was employed as the value of the *c* parameter will be discussed later.

Fig. 3 shows a typical example of the high resolution lattice image observed from the direction perpendicular to the fiber axis. Three kinds of fringe system for (001), (020) and {110} planes with the corresponding spacings of 7·3, 4·5 and 4·6 Å are clearly visible.

Fig. 4 shows an example of the damage by electron beam irradiation to a chrysotile fiber. The crystalline structure of the fresh specimen (*a* and *b*) changes rapidly to the amorphous state (*c* and *d*) on exposure to the intense electron beams necessary for imaging at the fairly high magnification. It was found that the crystallites usually became amorphous from the outer part toward the inner part of the fiber, leaving an irregular contour. However, the lattice parameters of a partially crystalline part still remain the same as that of a fresh fiber within the accuracy of measurement. It seems that the crystalline fibers are converted into amorphous silica and magnesia as a result of the dehydration induced by the electron beam irradiation.

On the other hand, in an experiment with heat treatment either in air or in a vacuum up to 550°C, the heat-treated fibers showed the same diffraction pattern and lattice image as those of the fresh fibers. Therefore, the damage due to electron irradiation does not seem to be a simple effect of the temperature rise of specimens caused by electron irradiation.

* The mean inner potential of chrysotile may be derived from the interval of split spots. A detailed analysis is in progress.

Table 1. *Lattice parameters of chrysotile reported by previous workers and the present author (clino-chrysotile)*

	Warren & Bragg	Warren & Herring	Aruja	Padurow	Whittaker	Brindley	Jagodzinski & Kunze	Whittaker & Zussman	Present author
a (Å)	14·66	7·33	14·62	7·36	14·65	5·33	5·33	5·34	5·30 ± 0·02
b (Å)	18·5	9·24	9·2	9·26	9·2	9·24	9·10	9·20	9·10 ± 0·05
c (Å)	5·33	5·33	5·32	5·33	5·33	7·33	7·33	14·65	7·32 ± 0·02
α	90°	90°	90°	92°50′	90°	90°	90°	90°	90°
β	93°16′	93°16′	93°12′	93°11′	93°7′	93°	93°16′	93°16′	93°
γ	90°	90°	90°	89°50′	90°	90°	90°	90°	90°
Date	1930	1942	1943	1950	1951	1952	1954	1956	1966

The lattice fringes of 7·3 Å spacing were always observed when the fibers were fresh, while the fringes of 4·5 Å spacing in the middle part of the fibers were not. The reason will be discussed later.

Fig. 5 shows an electron micrograph of a fiber in which the dislocations are seen in the encircled regions.

Fig. 6 is an electron micrograph showing a lattice image of para-chrysotile with the fiber axis in the [010] direction. This type of chrysotile was only rarely encountered and no isolated specimen was found. The identification by the electron diffraction pattern was for this reason not performed.

Specimens prepared by the sectioning method

Orientations of the sectioned chrysotile are distributed at random because the fibers are embedded in a random orientation. Chrysotile fibers sectioned perpendicularly to their axis were selected on the fluorescent screen and their micrographs were taken. A typical example is shown in Fig. 7. It is seen that most of the fibers are hollow tubes and the central holes are 50–80 Å in diameter. Two kinds of fringe, circumferential and radial, are clearly visible. In the crystallites *A* and *B* the circumferential fringes are visible continuously over the whole circumference corresponding to a nearly perfect excitation of Bragg reflection, while in the crystallites *C*, *D* and *E* the fringes are limited in a certain area because of an appreciable tilting of the fiber axis away from the direction of the illumination beam. *F* is a crystallite showing an unusual growth pattern. Other examples of crystallites showing such unusual growth will be presented later. The number of such unusual fibers is very small but seems to be slightly larger than that of para-chrysotile shown in Fig. 6.

Fig. 8 is an enlarged image of crystallites *A* and *B* of Fig. 7. The circumferential and radial fringes are traced with white ink to illustrate their behaviour. It is clearly seen that the circumferential fringes of 7·3 Å spacing are multi-spiral and the radial fringes of 4·5 Å spacing are not always straight but often zigzag in direction. It is also seen that the outer portions of the crystallites have been changed to an amorphous state by the electron beam irradiation.

Figs. 9 and 10 show other lattice images of crystallites observed from the fiber axis. Double spiral structures are clearly seen in Fig. 9, while the multi-spiral structures and also dislocations are visible in Fig. 10. It should be emphasized that all the crystallites observed have shown a spiral or multi-spiral structure but no concentric structure. The lattice is often distorted by the edge dislocations, and this results in some uncertainty in estimation of the lattice parameters.

Fig. 11 shows an electron diffraction pattern of the sectioned chrysotile observed from the direction parallel to the fiber axis. In this case, the diffraction spots or rings are not split, in contrast to the diffraction pattern of the specimen prepared by the suspension method shown in Fig. 1. This fact is easily understood if we take into account the uniform thickness of sectioned crystallites.

Fig. 12 shows other examples of crystallites showing unusual crystal growth. The crystallite in Fig. 12(*a*) has no central hole, while the crystallite in (*b*) shows partially terminated crystal planes.

Fig. 13 shows a thick crystallite containing partially terminated planes and also decentered holes similar to that in Fig. 12(*b*).

Discussion

The form of chrysotile fibers

The hollowed tabular forms of chrysotile fibers were revealed in more detail than before by the present observations on sectioned specimens. Most of the fibers were found to be really hollow tubes (Fig. 7). All the tubes observed are not simple cylindrical ones, but consist of spirally wound layers.

It is reasonable to consider that the deformation of the fibers by stress in the process of sectioning is negligible if we take into account the extreme thinness of the fiber diameter and also the favorable performance of embedding. Accordingly, it seems that the examples of the crystallites showing non-hollowed structures [Fig. 7, *F*, and Fig. 12(*a*)] represent real structures although their occurrence does not seem to be frequent. It was not confirmed whether para-chrysotile (Fig. 6), which was rarely encountered, is a hollow cylindrical fiber or simply a curved crystallite.

Lattice parameters and dislocation

The lattice parameters of clino-chrysotile estimated from the calibrated electron diffraction pattern are in good agreement with those found by some previous workers, as shown in Table 1. However, it should be noted from the observed lattice images that the lattice planes are distorted locally by dislocations existing with a fairly high density, which is estimated to be of the order of $10^{10} \sim 10^{11}$ cm^{-2}.

There are two possible ways to assign the value of the *c* parameter. Jagodzinski & Kunze (1954*a*,*b*) calculated the theoretically expected intensities of X-ray diffraction, and compared them with the experimental results by assuming the value 7·3 Å. Whittaker & Zussman (1956) carried out a similar procedure by using the value 14·6 Å.

The problem of whether the *c* parameter is 7·3 or 14·6 Å should be discussed in relation to the observed dislocation patterns. Now, if we assume the value of the *c* parameter to be 14·6 Å and an extra half plane of an edge dislocation, the observed lattice fringes of 7·3 Å spacing naturally correspond to the (002) plane and should include two extra lines on the position of the edge dislocation. Thus, the number of the observed extra lines should be always twice that of the actual extra lattice planes. In reality, however, many of the observed lattice images of the dislocations showed only one extra line as shown in Fig. 10, though two extra lines were observed in very rare cases as indicated by

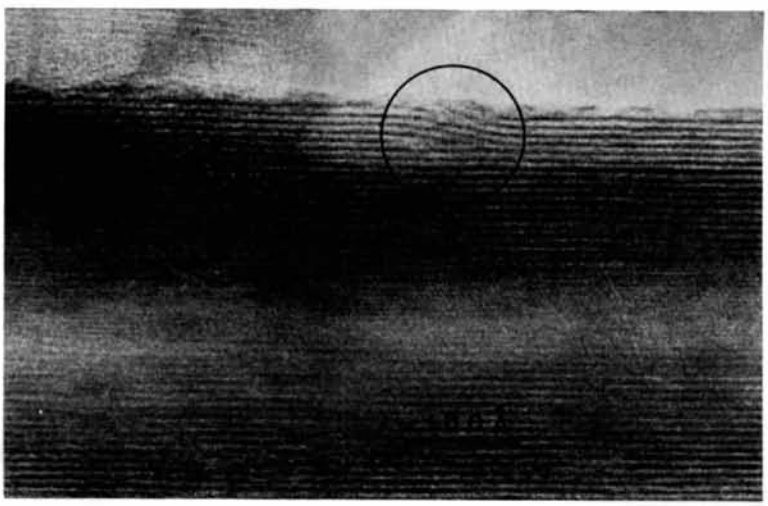

Fig. 5. Electron micrograph showing the dislocations in the (001) planes.

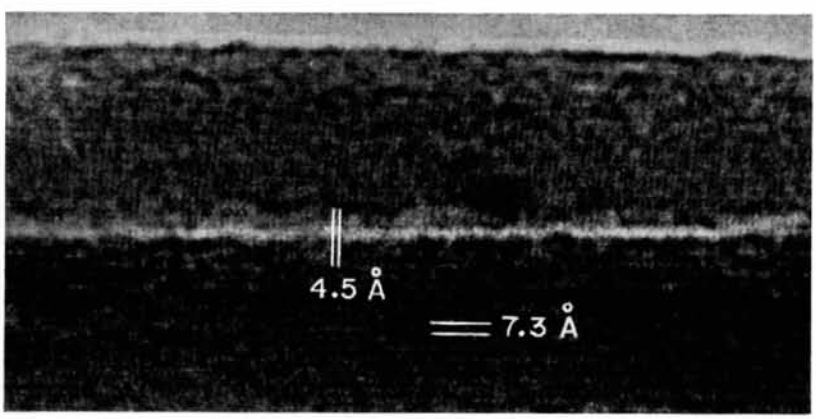

Fig. 6. Electron micrograph showing the lattice image of para-chrysotile which has the [010] direction as the fiber axis.

[*To face p.*706

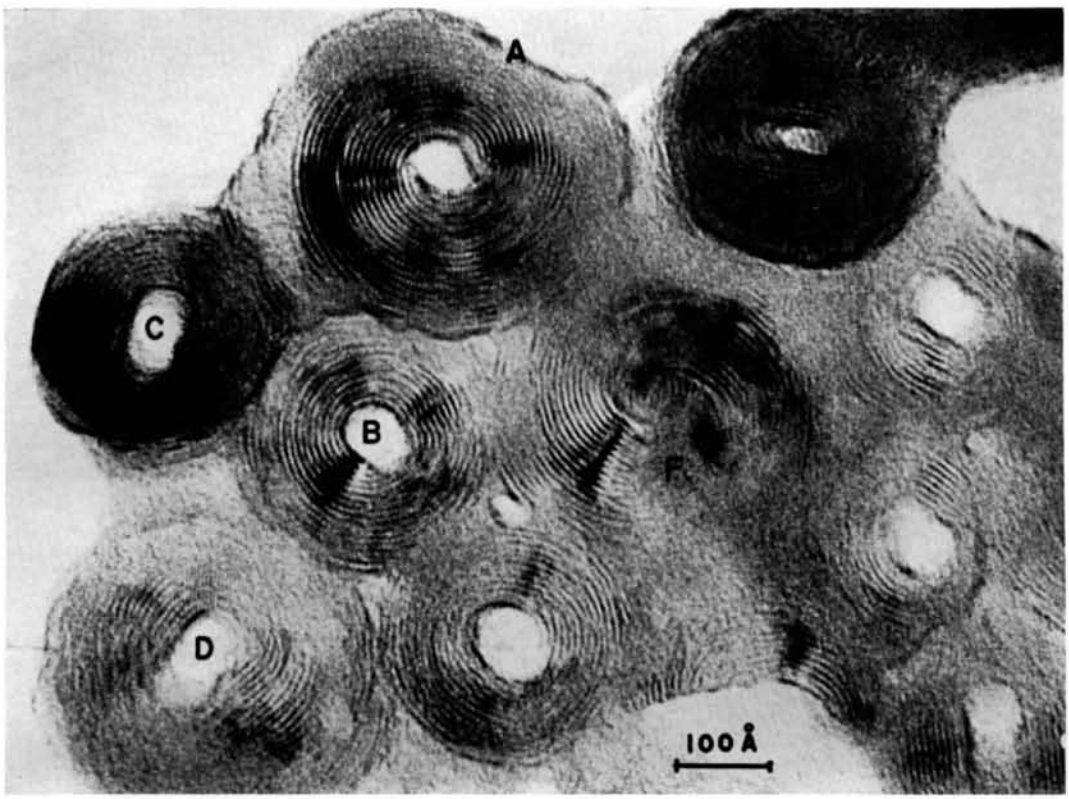

Fig. 7. A typical example of the lattice images of sectioned chrysotile observed from the direction parallel to the fiber axis.

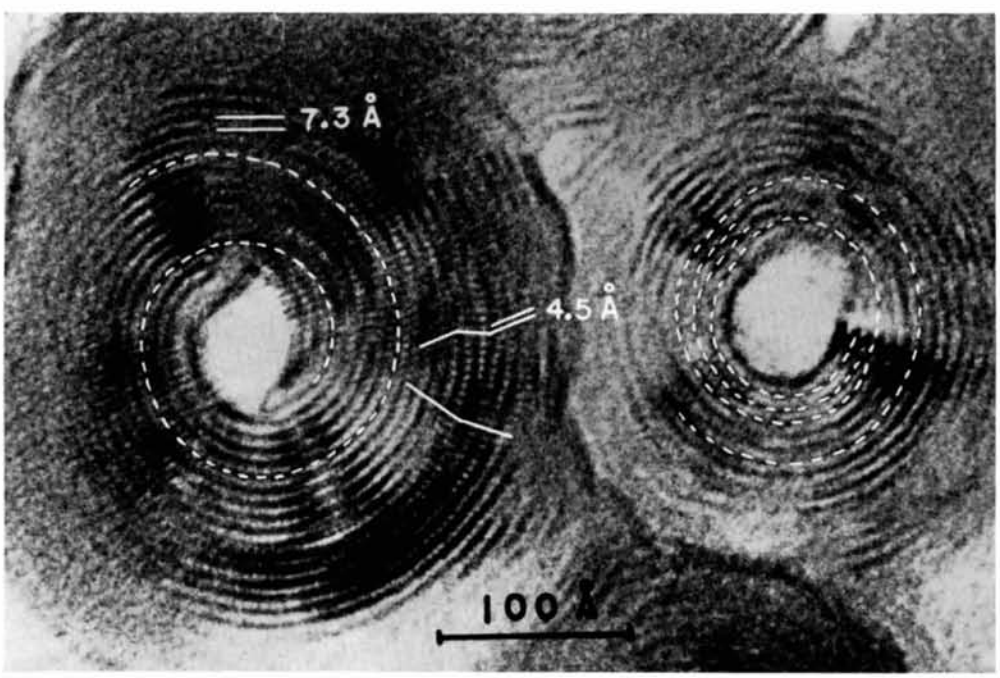

Fig. 8. Enlarged image of Fig. 7 (crystallites *A*, *B*) showing two kinds of fringe systems of the circumferential (001) and the radial (020) planes.

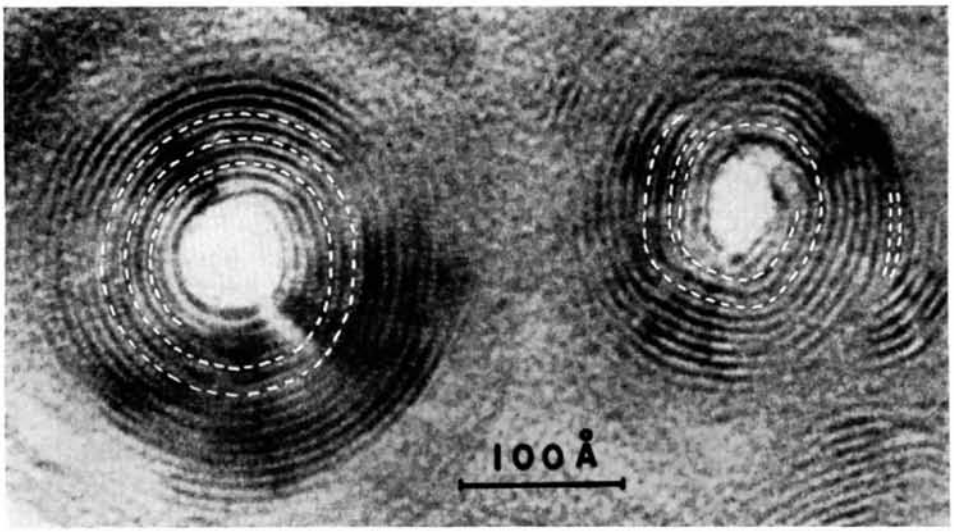

Fig. 9. Electron micrograph showing double spiral structures of the circumferential lattice planes.

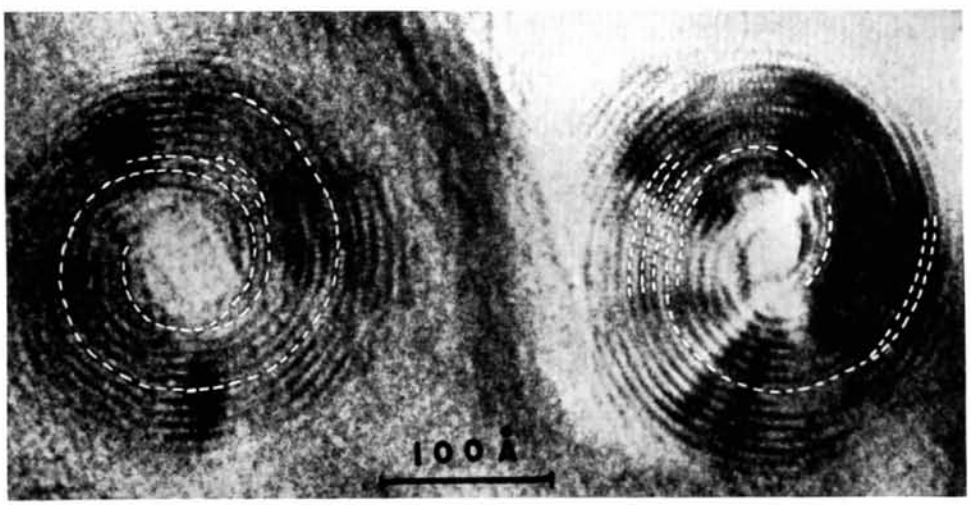

Fig. 10. Electron micrograph showing multi-spiral structures and dislocations of the circumferential lattice planes.

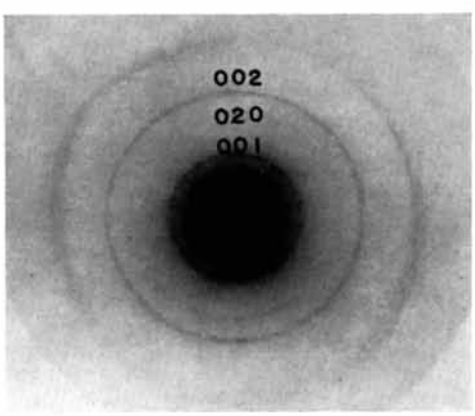

Fig. 11. Electron diffraction pattern of sectioned chrysotile observed from the direction parallel to the fiber axis.

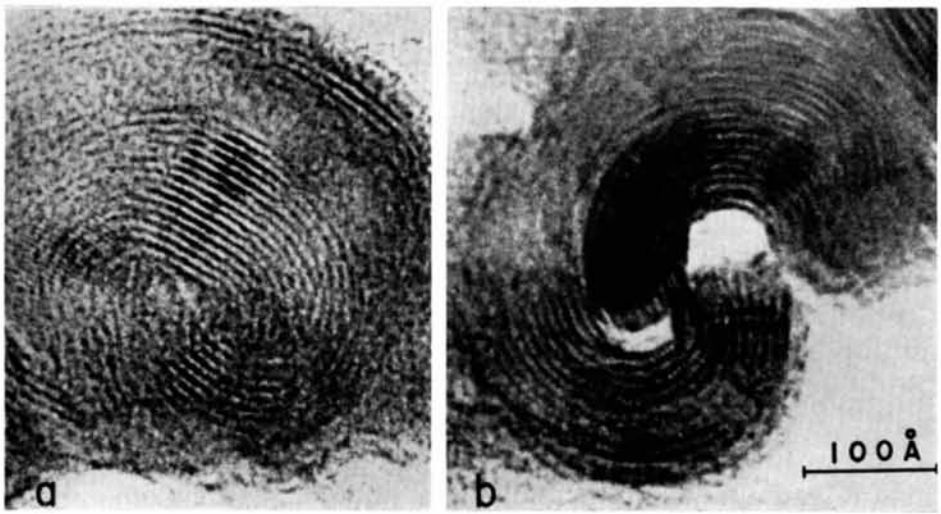

Fig. 12. Electron micrographs of cross-sections of chrysotile showing unusual growth patterns.

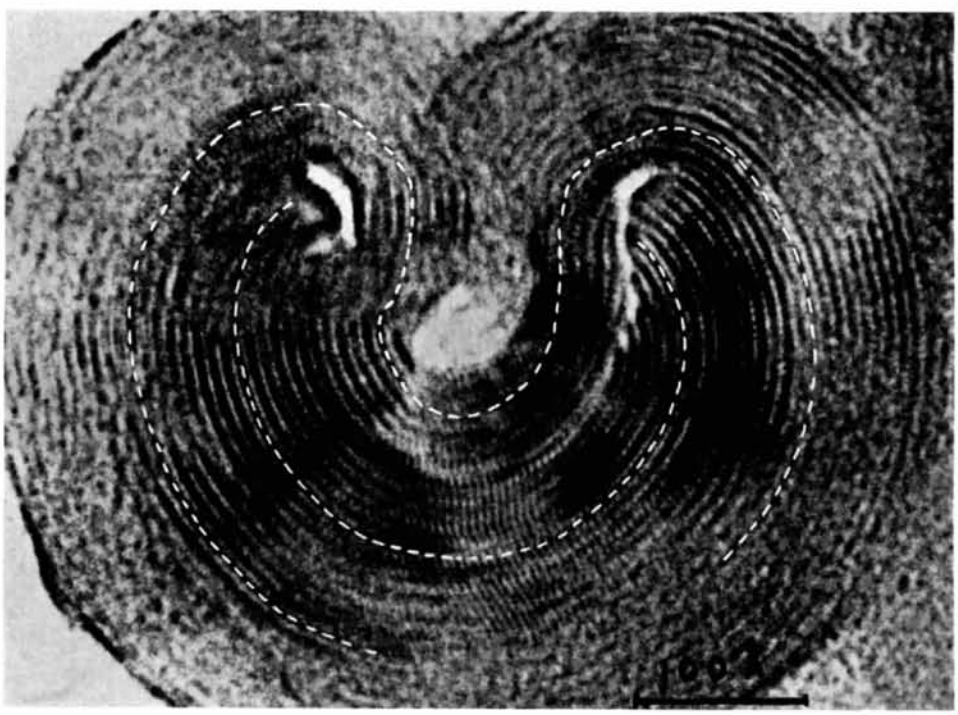

Fig. 13. Electron micrograph of a cross-section of chrysotile showing an unusual growth pattern.

[*To face p.*707

two dotted lines on the right edge of Fig. 9. In view of this experimental fact the repeating period of the unit cell in the **c** direction should be 7·3 Å rather than 14·6 Å.

The growth mechanism of chrysotile

Jagodzinski & Kunze (1954*c*) introduced the concept of axial, radial and coupled dislocations to explain the growth mechanism of hollow cylindrical fibers. The definitions of these dislocations are different from those of the so-called edge or screw dislocations but each of them allows an unlimited degree of growth. Their hypothesis was speculative though some indirect evidence was found in X-ray diffraction patterns. However, the present experimental facts, that the lattice images of the circumferential planes are always spiral, and also that dislocations are often observed, support the idea of growth mechanism by radial or coupled dislocations.

It is difficult to have the radial lattice fringes of 4·5 Å spacing over the whole sectioned area because the permissible angular deviation from the Bragg condition is very critical as compared with that for the 7·3 Å fringes. It is seen in the above observations that the radial fringes are not so perfectly straight and often change their direction. This fact explains why the fringes of 4·5 Å spacing are not always resolved in the middle part of the fiber when observed from the direction perpendicular to the fiber axis even with the highest resolution of the instrument.

There is a relation between the b and c parameters for circular cylindrical lattices, namely

$$nb = 2\pi c ,$$

where n is an integer. Substituting the values of b and c obtained in the present study, we have a value of $n = 5$, which indicates that the increment of the number of unit cells in the circumferential direction is five for each additional layer of radial direction. As the spacing of the observed radial fringes corresponds to the interplanar spacing of the (020) plane, the corresponding increment of radial fringes increases by 10 for each additional layer. Such a relation will hold approximately even in the case of the spiral lattices. Jagodzinski & Kunze (1954*a*) presented an idealized model in which the increment of unit cell was uniformly distributed over every circumferential layer. In reality, however, there is a variety in the appearance of the radial fringes as shown in the present results.

The existence of chrysotile fibers which are not hollow but solid had been expected because of a discrepancy between the calculated and experimental values of specific gravity (Pundsack, 1956; Whittaker, 1957). The existence of such fibers has been clearly demonstrated in the present work. Their proportion, however, is very small (perhaps a few %), contrary to the proposal by Whittaker (1957). Their growth mechanism is difficult to explain by the above-mentioned dislocation theory because they often show partially terminated multiple layers in a fiber. Further experiments on, for example, artificial chrysotile synthesized under controlled conditions by the lattice-image method, will be necessary to obtain more detailed information on the crystal growth mechanism.

The author is indebted to Prof. T. Hibi for valuable discussions and also greatly indebted to Prof. H. Fernández-Morán, The University of Chicago, for furnishing the specimens of chrysotile.

References

Aruja, E. (1943). Ph.D. Thesis, Cambridge.

Bates, T. F., Hildebrand, F. A. & Swineford, A. (1950). *Amer. Min.* **35**, 46.

Brindley, G. W. (1952). *X-ray Identification and Crystal Structures of Clay Minerals*, Chapter 2. London: Mineralogical Society.

Dowell, W. C. T. (1963). *Optik*, **20**, 535.

Fernández-Morán, H. (1966). *Proc. 6th Intern. Congr. Electron Microscopy, Kyoto.* Vol. I, p. 13.

Honjo, G. (1953). *J. Phys. Soc. Japan*, **8**, 776.

Honjo, G. & Mihama, K. (1954). *Acta Cryst.* **7**, 511.

Jagodzinski, H. & Kunze, G. (1954*a*). *Neues Jb. Min. Mh.* p. 95.

Jagodzinski, H. & Kunze, G. (1954*b*). *Neues Jb. Min. Mh.* p. 113.

Jagodzinski, H. & Kunze, G. (1954*c*). *Neues Jb. Min. Mh.* p. 137.

Komoda, T. (1966). *Japan J. Appl. Phys.* **5**, 452.

Padurow, N. N. (1950). *Acta Cryst.* **3**, 200.

Pundsack, F. L. (1956). *J. Phys. Chem.* **60**, 361.

Warren, B. E. & Bragg, W. L. (1930). *Z. Kristallogr.* **76**, 201.

Warren, B. E. & Herring, K. W. (1941). *Phys. Rev.* **59**, 925.

Whittaker, E. J. W. (1951). *Acta Cryst.* **4**, 187.

Whittaker, E. J. W. (1954). *Acta Cryst.* **7**, 827.

Whittaker, E. J. W. (1955). *Acta Cryst.* **8**, 571.

Whittaker, E. J. W. (1956). *Acta Cryst.* **9**, 855, 862, 865.

Whittaker, E. J. W. (1957). *Acta Cryst.* **10**, 149.

Whittaker, E. J. W. & Zussman, J. (1956). *Miner. Mag.* **31**, 107.

Yada, K. & Hibi, T. (1966). *Proc. 6th Intern. Congr. Electron Microscopy, Kyoto.* Vol. I, p. 25.

Zussman, J., Brindley, G. W. & Comer, J. J. (1957). *Amer. Min.* **42**, 133.